

Virulence-Associated Substitution D222G in the Hemagglutinin of 2009 Pandemic Influenza A(H1N1) Virus Affects Receptor Binding^{∇‡}

Salin Chutinimitkul,^{1†} Sander Herfst,^{1†} John Steel,² Anice C. Lowen,² Jianqiang Ye,³ Debby van Riel,¹ Eefje J. A. Schrauwen,¹ Theo M. Bestebroer,¹ Björn Koel,¹ David F. Burke,⁴ Kyle H. Sutherland-Cash,⁵ Chris S. Whittleston,⁵ Colin A. Russell,^{4,9} David J. Wales,⁵ Derek J. Smith,^{1,4,9} Marcel Jonges,⁶ Adam Meijer,⁶ Marion Koopmans,⁶ Guus F. Rimmelzwaan,¹ Thijs Kuiken,¹ Albert D. M. E. Osterhaus,¹ Adolfo García-Sastre,^{2,7,8} Daniel R. Perez,³ and Ron A. M. Fouchier^{1*}

National Influenza Center and Department of Virology, Erasmus Medical Center, Rotterdam, Netherlands¹; Department of Microbiology, Mount Sinai School of Medicine, New York, New York²; Department of Veterinary Medicine, University of Maryland, College Park, Maryland³; Department of Zoology, University of Cambridge, Downing Street, Cambridge CB2 3EJ, United Kingdom⁴; University Chemical Laboratories, University of Cambridge, Lensfield Road, Cambridge CB2 1EW, United Kingdom⁵; National Institute for Public Health and the Environment, Laboratory for Infectious Diseases and Screening, Bilthoven, Netherlands⁶; Department of Medicine, Division of Infectious Diseases, Mount Sinai School of Medicine, New York, New York⁷; Global Health and Emerging Pathogens Institute, Mount Sinai School of Medicine, New York, New York⁸; and Fogarty International Center, National Institutes of Health, Bethesda, Maryland⁹

Received 27 May 2010/Accepted 1 September 2010

The clinical impact of the 2009 pandemic influenza A(H1N1) virus (pdmH1N1) has been relatively low. However, amino acid substitution D222G in the hemagglutinin of pdmH1N1 has been associated with cases of severe disease and fatalities. D222G was introduced in a prototype pdmH1N1 by reverse genetics, and the effect on virus receptor binding, replication, antigenic properties, and pathogenesis and transmission in animal models was investigated. pdmH1N1 with D222G caused ocular disease in mice without further indications of enhanced virulence in mice and ferrets. pdmH1N1 with D222G retained transmissibility via aerosols or respiratory droplets in ferrets and guinea pigs. The virus displayed changes in attachment to human respiratory tissues *in vitro*, in particular increased binding to macrophages and type II pneumocytes in the alveoli and to tracheal and bronchial submucosal glands. Virus attachment studies further indicated that pdmH1N1 with D222G acquired dual receptor specificity for complex α 2,3- and α 2,6-linked sialic acids. Molecular dynamics modeling of the hemagglutinin structure provided an explanation for the retention of α 2,6 binding. Altered receptor specificity of the virus with D222G thus affected interaction with cells of the human lower respiratory tract, possibly explaining the observed association with enhanced disease in humans.

In April 2009, the H1N1 influenza A virus of swine origin was detected in humans in North America (9, 12, 42). Evidence for its origin came from analyses of the viral genome, with six gene segments displaying the closest resemblance to American “triple-reassortant” swine viruses and two to “Eurasian-lineage” swine viruses (13, 42). After this first detection in humans, the virus spread rapidly around the globe, starting the first influenza pandemic of the 21st century. The 2009 pandemic influenza A(H1N1) virus (pdmH1N1) has been relatively mild, with a spectrum of disease ranging from subclinical infections or mild upper respiratory tract illness to sporadic cases of severe pneumonia and acute respiratory distress syndrome (3, 11, 27, 29, 30, 37). Overall, the case-fatality rate

during the start of the pandemic was not significantly higher than in seasonal epidemics in most countries. However, a marked difference was observed in the case-fatality rate in specific age groups, with seasonal influenza generally causing highest mortality in elderly and immunocompromised individuals, and the pdmH1N1 affecting a relatively large proportion of (previously healthy) young individuals (3, 11, 27, 29, 30, 37).

Determinants of influenza A virus virulence have been mapped for a wide variety of zoonotic and pandemic influenza viruses to the polymerase genes, hemagglutinin (HA), neuraminidase (NA), and nonstructural protein 1 (NS1). Such virulence-associated substitutions generally facilitate more efficient replication in humans via improved interactions with host cell factors. Since most of these virulence-associated substitutions were absent in the earliest pdmH1N1s, it has been speculated that the virus could acquire some of these mutations, potentially resulting in the emergence of more pathogenic viruses. Such virulence markers could be acquired by gene reassortment with cocirculating influenza A viruses, or by mutation. The influenza virus polymerase genes, in particular PB2, have been shown to be important determinants of the virulence

* Corresponding author. Mailing address: Department of Virology, Erasmus Medical Center Rotterdam, P.O. Box 2040, 3000 CA Rotterdam, Netherlands. Phone: 31 10 7044066. Fax: 31 10 7044760. E-mail: r.fouchier@erasmusmc.nl.

† S.C. and S.H. contributed equally to this study.

‡ Supplemental material for this article may be found at <http://jvi.asm.org/>.

[∇] Published ahead of print on 15 September 2010.

of the highly pathogenic avian influenza (HPAI) H5N1 and H7N7 viruses and the transmission of the 1918 H1N1 Spanish influenza virus (17, 26, 34, 51). One of the most commonly identified virulence markers to date is E627K in PB2. The glutamic acid (E) residue is generally found in avian influenza viruses, while human viruses have a lysine (K), and this mutation was described as a determinant of host range *in vitro* (48). Given that all human and many zoonotic influenza viruses of the last century contained 627K, it was surprising that the pdmH1N1 had 627E. In addition, an aspartate (D)-to-asparagine (N) substitution at position 701 (D701N) of PB2 has previously been shown to expand the host range of avian H5N1 virus to mice and humans and to increase virus transmission in guinea pigs (26, 46). Like E627K, D701N was absent in the genome of pdmH1N1. Thus, the pdmH1N1 was the first known human pandemic virus with 627E and 701D, and it has been speculated that pdmH1N1 could mutate into a more virulent form by acquiring one of these mutations or both. Recently, it was shown that neither E627K nor D701N in PB2 of pdmH1N1 increased its virulence in ferrets and mice (18). The PB1-F2 protein has previously also been associated with high pathogenicity of the 1918 H1N1 and HPAI H5N1 viruses (8). The PB1-F2 protein of the pdmH1N1 is truncated due to premature stop codons. However, restoration of the PB1-F2 reading frame did not result in viruses with increased virulence (15). The NS1 protein of pdmH1N1 is also truncated due to a stop codon and, as a result, does not contain a PDZ ligand domain that is involved in cell-signaling pathways and has been implicated in the pathogenicity of 1918 H1N1 and HPAI H5N1 viruses (5, 8, 21). Surprisingly, restoration of a full-length version of the NS1 gene did not result in increased virulence in animal models (16). Mutations affecting virulence and host range have further frequently been mapped to hemagglutinin (HA) and neuraminidase (NA) in relation to their interaction with α 2,3- or α 2,6-linked sialic acids (SAs), the virus receptors on host cells (17, 32, 35, 50). The HA gene of previous pandemic viruses incorporated substitutions that allow efficient attachment to α 2,6-SAs—the virus receptor on human cells—compared to ancestral avian viruses that attach more efficiently to α 2,3-SAs (35, 47, 50).

To search for mutations of potential importance to public health, numerous laboratories performed genome sequencing of pdmH1N1s, resulting in the real-time accumulation of information on emergence of potential virulence markers. Of specific interest were reports on amino acid substitutions from aspartic acid (D) to glycine (G) at position 222 (position 225 in H3) in HA of pdmH1N1. This substitution was observed in a fatal case of pdmH1N1 infection in June 2009 in the Netherlands (M. Jonges et al., unpublished data). Between July and December 2009, viruses from 11 (18%) of 61 cases with severe disease outcome in Norway have also been reported to harbor the D222G substitution upon direct sequencing of HA in clinical specimens. Such mutant viruses were not observed in any of 205 mild cases investigated, and the frequency of detection of this mutation was significantly higher in severe cases than in mild cases (23). In Hong Kong, the D222G substitution was detected in 12.5% (6) and 4.1% (31) of patients with severe disease and in 0% of patients with mild disease, in two different studies without prior propagation in embryonated chicken eggs. In addition to Norway and Hong Kong, the mutation has

been detected in Brazil, Japan, Mexico, Ukraine, and the United States (56). Thus, D222G in HA could be the first identified “virulence marker” of pdmH1N1. pdmH1N1 with D222G in HA have not become widespread in the population, although they were detected in several countries. However, D222G in HA is of special interest, since it has also been described as the single change in HA between two strains of the “Spanish” 1918 H1N1 virus that differed in receptor specificity (47). Furthermore, upon propagation in embryonated chicken eggs, pdmH1N1 can acquire the mutation rapidly, presumably because it results in virus adaptation to avian (α 2,3-SAs) receptors (49). The presence of the substitution in pdmH1N1s in the human population and its potential association with more severe disease prompted us to test its effect on pdmH1N1 receptor binding, replication, antigenic properties, and pathogenesis and transmission in animal models.

MATERIALS AND METHODS

Cells and viruses. Madin-Darby Canine kidney (MDCK) cells were cultured in Eagle's minimum essential medium (EMEM; Cambrex, Heerhugowaard, Netherlands) supplemented with 10% fetal calf serum (FCS), 100 IU of penicillin/ml, 100 μ g of streptomycin/ml, 2 mM glutamine, 1.5 mg of sodium bicarbonate (Cambrex/ml, 10 mM HEPES (Cambrex), and nonessential amino acids (MP Biomedicals Europe, Illkirch, France). 293T cells were cultured in Dulbecco's modified Eagle's medium (Cambrex) supplemented with 10% FCS, 100 IU of penicillin/ml, 100 mg of streptomycin/ml, 2 mM glutamine, 1 mM sodium pyruvate, and nonessential amino acids. Influenza virus A/Netherlands/602/2009 was isolated from the first patient with pdmH1N1 virus infection in the Netherlands (33). All eight gene segments of this virus were amplified by reverse transcription-PCR, cloned in a modified version of the bidirectional reverse genetics plasmid pHW2000 (10, 19), and subsequently used to generate recombinant virus by reverse genetics as described elsewhere (10). The mutations of interest (D222E and D222G) were introduced in the HA gene segment by using the QuikChange multi site-directed mutagenesis kit (Stratagene, Leusden, Netherlands) according to the instructions of the manufacturer. D222G was selected based on the association with increased virulence, whereas D222E was included as a control, since it was observed frequently in circulating pdmH1N1s. Recombinant viruses NL602-WT, NL602-D222E, and NL602-D222G were rescued in 293T cells and propagated in MDCK cells. Virus titers were determined in MDCK cells as described below. The presence of each mutation and the absence of undesired mutations were confirmed by sequencing the HA gene of the recombinant viruses.

Modified TRBC hemagglutination assay. Modified turkey red blood cells (TRBCs) were prepared as described previously (36) with minor modifications. Briefly, α 2,3-, α 2,6-, α 2,8-, and α 2,9-linked SAs were removed from the surface of TRBCs by incubating 62.5 μ l of 20% TRBCs in phosphate-buffered saline (PBS) with 50 mU of *Vibrio cholerae* NA (VCNA; Roche, Almere, Netherlands) in 8 mM calcium chloride at 37°C for 1 h. The removal of sialic acids was confirmed by demonstrating the complete loss of hemagglutination of the TRBCs by control influenza A viruses. Subsequently, resialylation was performed using 0.5 mU α 2,3-(N)-sialyltransferase (Calbiochem, CA) or 2 mU of α 2,6-(N)-sialyltransferase (Japan Tobacco, Inc., Shizuoka, Japan) and 1.5 mM cytidine monophospho-N-acetylneuraminic (CMP) sialic acid (Sigma-Aldrich, Zwijndrecht, Netherlands) at 37°C in 75 μ l for 2 h to produce α 2,3-TRBCs and α 2,6-TRBCs, respectively. After washing, the TRBCs were resuspended in PBS containing 1% bovine serum albumin to a final concentration of 0.5% TRBCs. Resialylation was confirmed by hemagglutination assay with human and avian influenza viruses with known receptor specificities for α 2,6 and α 2,3 SAs, respectively. The receptor specificity of the mutant viruses was tested by performing a standard hemagglutination assay with the modified TRBCs. In brief, serial 2-fold dilutions of virus in PBS were made in a 50- μ l volume; 50 μ l of 0.5% TRBCs was added, followed by incubation for 1 h at 4°C before the hemagglutination titer was determined.

Virus titrations. Virus titers in virus stocks, nasal and throat swabs, homogenized organ samples or samples from inoculated MDCK cells were determined by endpoint titration in MDCK cells. MDCK cells were inoculated with 10-fold serial dilutions of each sample, washed 1 h after inoculation with PBS, and cultured in 200 μ l of infection medium, consisting of EMEM supplemented with

100 IU of penicillin/ml, 100 µg of streptomycin/ml, 2 mM glutamine, 1.5 mg of sodium bicarbonate/ml, 10 mM HEPES, nonessential amino acids, and 17.5 µg of trypsin/ml. At 3 days after inoculation, supernatants of infected cell cultures were tested for agglutinating activity using turkey erythrocytes as an indicator of virus replication in the cells. Infectious virus titers were calculated from four replicates by the method of Spearman-Kärber (22).

Replication curves. Replication curves were generated by inoculating MDCK cells at a multiplicity of infection (MOI) of 0.01 50% tissue culture infectious doses (TCID₅₀) per cell. Supernatants were sampled at 6, 12, 24, and 48 h postinfection, and the virus titers in these supernatants were determined by means of endpoint titration in MDCK cells as described above.

Animal experiments. For pathogenesis studies performed in mice (*Mus musculus*), experiments were performed in accordance with the guidelines of the University of Maryland Institutional Animal Care and Use Committee. Groups of six 5-week-old female BALB/c mice were inoculated intranasally with 2.5×10^6 TCID₅₀ of influenza virus, and body weights were recorded daily until 14 days postinfection (dpi) as an indicator of disease. In a separate experiment, three animals from each group were euthanized at 3 and 5 dpi, and the lungs were collected and subsequently homogenized for virus titration. Virus titers were determined by endpoint titration in MDCK cells as described above.

For pathogenesis and transmission studies performed in ferrets (*Mustella putorius furo*), the experiments were approved by an independent Animal Ethics Committee contracted by Erasmus MC Rotterdam. Healthy young adult out-breed female ferrets between 6 and 12 months old weighing 0.8 to 1.5 kg were tested for the absence of antibodies against seasonal H1N1 and H3N2 influenza viruses and the pdmH1N1 virus by a hemagglutination inhibition (HI) assay. Ferrets were anesthetized via intramuscular injection of a ketamine-metomidine mixture prior to inoculation (reversed with atipamezole) and with ketamine prior to nose and throat swab collection. To study pathogenesis, groups of six ferrets were inoculated intranasally with 10^6 TCID₅₀ of influenza virus divided over both nostrils (i.e., 2×250 µl). Throat and nasal swabs were collected daily to determine virus excretion from the upper respiratory tract. Animals were observed for clinical signs and weighed daily as an indicator of disease. Three animals from each group were euthanized at 3 and 7 dpi, and the nasal turbinates, trachea, lungs, livers, spleens, kidneys, colons, and brains were collected to study virus distribution. In ferret transmission experiments, four animals were housed individually in transmission cages and inoculated intranasally with 10^6 TCID₅₀ of influenza virus divided over both nostrils (2×250 µl). At 1 dpi, four naive ferrets were individually placed in a transmission cage adjacent to an inoculated ferret, separated by two stainless steel grids, to allow airflow from the inoculated to the naive ferret but to prevent direct contact and fomite transmission. Nasal and throat swabs were collected at 0, 1, 2, 3, 5, and 7 dpi from inoculated ferrets and at 0, 1, 2, 3, 5, and 7 days postexposure (dpe) for the naive animals. Inoculated ferrets were euthanized at 7 dpi, and naive ferrets that were shedding virus by 7 dpe were also euthanized. Naive animals that remained negative for virus excretion throughout the experiment were euthanized at 15 dpe, and a blood sample was collected for serology. Virus titers in collected swabs and tissue homogenates were determined by means of endpoint titration in MDCK cells as described above (33).

For transmission studies performed in guinea pigs (*Cavia porcellus*), experiments were performed in accordance with the guidelines of the Mount Sinai School of Medicine Institutional Animal Care and Use Committee. Female Hartley strain guinea pigs weighing 300 to 350 g were obtained from Charles River Laboratories (Wilmington, MA). Guinea pigs were anesthetized through intramuscular injection of a ketamine-xylazine mixture (30 and 2 mg/kg, respectively) prior to inoculation and nasal wash collection. Four guinea pigs were inoculated intranasally with 10^4 TCID₅₀ of influenza virus in 300 µl of PBS. Exposure of naive guinea pigs to inoculated guinea pigs was initiated at 1 dpi and continued for 7 days. Nasal washings were collected from animals on 2, 4, 6, and 8 dpi or dpe. Aerosol transmission experiments were performed within a Caron environmental test chamber (model 6030) set to 20°C and 20% relative humidity. Cages placed within the chamber were open at the top and at one side such that air exchange occurred among all eight cages; thus, direct pairings of infected and exposed animals were not made. To prevent aberrant cross-contamination between cages, exposed animals were handled before inoculated animals and gloves were disinfected between cages.

Immunohistochemistry. Samples for histological examination were stored in 10% neutral-buffered formalin, embedded in paraffin, sectioned at 4 µm, and stained with an immunohistochemical method using a mouse monoclonal antibody against the nucleoprotein of influenza A virus (39). Goat anti-mouse IgG2a HRP directed against the primary antibody was used as a secondary antibody. The peroxidase activity of the conjugate was revealed by using 3-amino-9-ethylcarbazole (AEC; Sigma-Aldrich), resulting in a red precipitate.

Virus purification and labeling. Viruses were purified and labeled with fluorescein isothiocyanate (FITC; Sigma-Aldrich) as described previously (52). Briefly, virus stocks prepared in MDCK cells were concentrated and purified by using sucrose gradients, inactivated by dialysis against 0.1% formalin, and labeled with an equal volume of 0.1 mg of FITC/ml.

Virus histochemistry on tissue sections. The paraffin-embedded human respiratory tract tissue sections were obtained from the Department of Pathology, Erasmus Medical Center. The paraffin-embedded animal tissue sections were obtained from the Department of Virology, Erasmus Medical Center. All selected tissues were without histological lesions or evidence of respiratory tract infection. Tissues from three individuals of each species were analyzed. Virus histochemistry was performed as described previously (52). Briefly, formalin-fixed, paraffin-embedded tissues were deparaffinized with xylene and rehydrated with graded alcohol. FITC-labeled influenza viruses (50 to 100 hemagglutinating units) were incubated with tissues overnight at 4°C. The FITC label was detected with a peroxidase-labeled rabbit anti-FITC antibody (Dako, Heverlee, Belgium), and the signal was amplified with a tyramide signal amplification system (Perkin-Elmer, Groningen, Netherlands) according to the manufacturer's instructions. Peroxidase was revealed with 3-amino-9-ethyl-carbazole (Sigma-Aldrich), and tissues were counterstained with hematoxylin and embedded in glycerol-gelatin (Merck, Darmstadt, Germany). Attachment of influenza virus to tissues was visible as granular to diffuse red staining.

HI assay. Hemagglutination inhibition (HI) assays using postinfection ferret and rabbit antisera were performed to compare the antigenic properties of influenza A virus isolates as described previously (44). All antisera were treated overnight with receptor-destroying enzyme and subsequently incubated at 56°C for 1 h. Twofold serial dilutions of each antiserum, starting at a 1:20 dilution, were tested for their ability to inhibit the agglutination of turkey erythrocytes by four hemagglutinating units of influenza A virus. All HI assays were performed in duplicate.

In silico generation of glycan structures. The three-sugar glycan, NeuAcα2,6Galβ1-4GlcNAcβ1 with a methyl cap attached to the O1 atom of the terminal sugar, was constructed and parameterized using LEaP (4) with Glycam06c parameters (24) before being subjected to geometry optimization using GMIN (54). Partial charges for the glycan atoms were calculated by using GAMESS (41) with a 6-31G* basis set and the restricted electrostatic potential method (1). These charges were used for a final minimization before docking into the protein.

In silico prediction of initial HA-glycan complex. A model of the structure of the HA of NL602 was built by using MODELLER (40) based upon the crystal structure of HA of the H1N1 1918 A/SouthCarolina/1/18 virus (PDB code 1RUZ). The D222G mutation was introduced by using the program Andante (45). The glycan was docked into the binding site of the NL602 and the 1918 A/SouthCarolina/1/18 HA structure based upon the experimentally determined crystal structure of swine 1930 H1N1 (PDB code 1RVT). Several strategies were then used to explore the docking of the glycan within the binding pocket. Initial glycan conformations were produced with the phi angle of the glycosidic bond between the second and third sugars set to either 0° or 180°. Exploration of alternative side chain conformations of amino acids within the binding pocket was performed by using a rotamer search (45). Molecular dynamics simulations and global optimization by basin-hopping (55) were then used, as described below, to produce optimized docked conformations for each set of initial docked complexes.

Molecular dynamics simulations. Molecular dynamics simulations of each complex were performed by using GROMACS (28) with the AMBER ff99SB force field. Each model was placed in an 80-by-80-by-80 Å box containing approximately 20,000 TIP3P water molecules and minimized for 1,000 BFGS steps to remove any unfavorable contacts. The system was equilibrated by heating the complex to 306 K. Production runs were then performed for 1 ns at neutral pH. All glutamate and aspartate residues were therefore negatively charged, while lysine and arginine were positively charged and histidines were neutral. The system charge was neutralized by adding an appropriate number of counterions (Na⁺ or Cl⁻). The particle mesh Ewald method was used to compute long-range electrostatic interactions, using a 1.0-Å grid spacing and a fourth-order spline for interpolation. The nonbonded cutoff was set to 9.0 Å, and the SHAKE algorithm was used to constrain all bonds involving hydrogen atoms. A time step of 2.0 fs was used in all simulations, and coordinates (snapshots) were saved every 20 ps. Periodic boundary conditions were applied throughout. Simulations for each complex were repeated 10-fold with different initial starting velocities. The molecular dynamics simulations were performed using the University of Cambridge CAMGRID computing cluster (2).

Basin-hopping global optimization. Local minima of low potential energy were identified by using the basin-hopping approach (55) (a variant of Monte Carlo with minimization) as implemented in the program GMIN (54). In this

method, every step consisting of a change in the current coordinates is followed by local minimization of the resulting structure. A Metropolis criterion based on the potential energies of the old and new minima is then applied to determine whether to accept or reject the move to the new local minimum. To allow efficient sampling of possible receptor conformations, a hybrid step-taking scheme was used. This scheme consisted of a short, high-temperature (450 K) molecular dynamics trajectory, using the Generalized Born implicit solvent model (igb = 1), followed by a rigid body rotation of the sugar about its center of coordinates. Finally, a small random perturbation was applied to all atoms of the receptor.

Classification of binding modes. The different binding modes described were defined according to separation of the center of mass of the backbone atoms of residue 224 and the center of mass of the O2 and O3 atoms of the α 2,6-SA galactose sugar. Those where this distance was $<6 \text{ \AA}$ were classified as mode 1, those where the distance was $>7 \text{ \AA}$ were classified as mode 2, and others were classified as intermediate.

Hydrogen bond analysis. Hydrogen bonds were characterized using the default settings (3.5- \AA cutoff distance with no cutoff angle) for ptraj as distributed with AmberTools 1.1 (4). The presence of each hydrogen bond of interest was recorded for every snapshot generated during molecular dynamics simulations. The percentage of structures containing these hydrogen bonds was calculated over all repeats of a given strain. The analysis was repeated separately for structures classified as mode 1, mode 2, and intermediate as described above.

RESULTS

***In vitro* replication kinetics.** Recombinant viruses with or without the D222E and D222G substitutions in HA were generated in 293T cells by reverse genetics using the prototype pdmH1N1 virus A/Netherlands/602/2009 as the genetic backbone. D222G was selected because it may be associated with increased virulence, and D222E was chosen as a control because it was observed in a relatively large proportion of pdmH1N1s without evidence for association with increased virulence. Viruses produced in 293T cells were propagated and titrated in MDCK cells. Subsequently, MDCK cells were inoculated at an MOI of 0.01, after which supernatants were harvested at fixed time points and the virus titers were determined in MDCK cells (see Fig. S1 in the supplemental material). The replication kinetics of the wild-type virus and the two mutant viruses were similar. NL602-D222G replicated to slightly lower titers in the first 24 h after inoculation, with <10 -fold differences in virus titers, which is not statistically significant.

Pathogenesis experiments in ferrets. To investigate potential differences in virulence, groups of six ferrets were inoculated intranasally with 10^6 TCID₅₀ of NL602-WT, NL602-D222E, or NL602-D222G. The animals were weighed daily as an indicator of disease. The mean maximum weight loss was 9 to 10.5% over the 7-day period, with no statistically significant differences among the groups (Fig. 1A) (see Fig. S2 in the supplemental material). No marked differences were observed for clinical parameters such as lethargy, ruffled fur, interest in food, and runny nose between the groups. Nose and throat swabs were collected from inoculated animals daily, and virus titers were determined by endpoint titration in MDCK cells. Virus shedding was observed from 1 dpi onward and continued until 7 dpi from both the noses and throats of ferrets inoculated with the three viruses (Fig. 1B and C). Overall, only minor differences in virus shedding—which did not reach statistical significance—were observed among the groups. At 3 and 7 dpi, three ferrets from each group were euthanized, and the nasal turbinates, trachea, lungs, brains, livers, spleens, kidneys, and colons were collected for virological examination. Parts of the collected tissues were homogenized, and virus

titers were determined by titration in MDCK cells. Virus was detected in the nasal turbinates, tracheas, and lungs at 3 dpi in 3/3 animals inoculated with each virus, but not in the other organs (see Table S1 in the supplemental material). The virus titers recovered from the respiratory tract tissues did not reveal remarkable differences. At 7 dpi, virus was only detected in the lungs of one of three ferrets inoculated with NL602-WT, in the nasal turbinates of two of three animals inoculated with NL602-WT and NL602-D222G, and in the trachea of one of three animals inoculated with NL602-WT and NL602-D222E. At 7 dpi, virus titers were generally lower than at 3 dpi, suggesting virus clearance in this animal model over time. Sequence analyses of HA of viruses isolated from the noses and lungs of infected ferrets were performed to confirm that the viruses did not change by mutation. Influenza virus antigen expression in tissue sections of the nasal turbinates and lungs of ferrets inoculated with NL602-WT, NL602-D222E, and NL602-D222G collected at 3 dpi were stained with a monoclonal antibody against influenza A virus nucleoprotein and counterstained with hematoxylin and eosin. Both nasal epithelial cells and bronchiolar epithelial cells expressed influenza virus antigen. No differences in influenza virus antigen expression were observed between the three groups of ferrets (see Fig. S3 in the supplemental material). Thus, there were no marked differences in pathogenicity and virus shedding between the ferrets infected with the wild-type and mutant H1N1 viruses tested.

Pathogenesis experiments in mice. To investigate the pathogenesis in mice, groups of five or six BALB/c mice were inoculated intranasally with 2.5×10^6 TCID₅₀ of each virus and weighed daily as an indicator of disease (Fig. 1D) (see Fig. S4 in the supplemental material). In the first 4 days, mice in all three groups lost body weight at the same rate. At 4 dpi, several mice in each group showed more than 25% body weight loss and were euthanized for ethical reasons, and at 7 dpi all mice were euthanized (Fig. 1E). At 4 and 5 dpi, all mice inoculated with NL602-D222G experienced difficulties in opening their eyes, either unilaterally or bilaterally, and were more sensitive to light, in contrast to mice inoculated with NL602-WT and NL602-D222E. Virus was isolated from the eyes of only one of three mice tested and at a very low titer of 0.7 TCID₅₀/ml. Other clinical signs were similar in the three groups. In parallel, groups of six mice were inoculated intranasally with 2.5×10^6 TCID₅₀ of the three viruses, and the lung virus titers were determined at 3 and 5 dpi by titration of lung homogenates in MDCK cells. The titers for NL602-D222E- and NL602-D222G-inoculated groups were $\sim 0.3 \log_{10}$ TCID₅₀ higher than for NL602-WT at 3 dpi. At 5 dpi, the lung virus titers for NL602-D222E- and NL602-D222G-inoculated groups were $0.3 \log_{10}$ TCID₅₀ lower than for the NL602-WT group (Fig. 1F). Although there were thus some differences in virus replication and pathogenicity between the groups inoculated with the wild-type and mutant viruses, the differences were relatively small.

Transmission experiments in ferrets. Aerosol or respiratory droplet transmission of the three viruses was tested in the ferret model. Four individually housed ferrets were inoculated with each virus, and naive animals were placed in a cage adjacent to each inoculated ferret at 1 dpi. The experimental setup was designed to prevent transmission via contact, but to

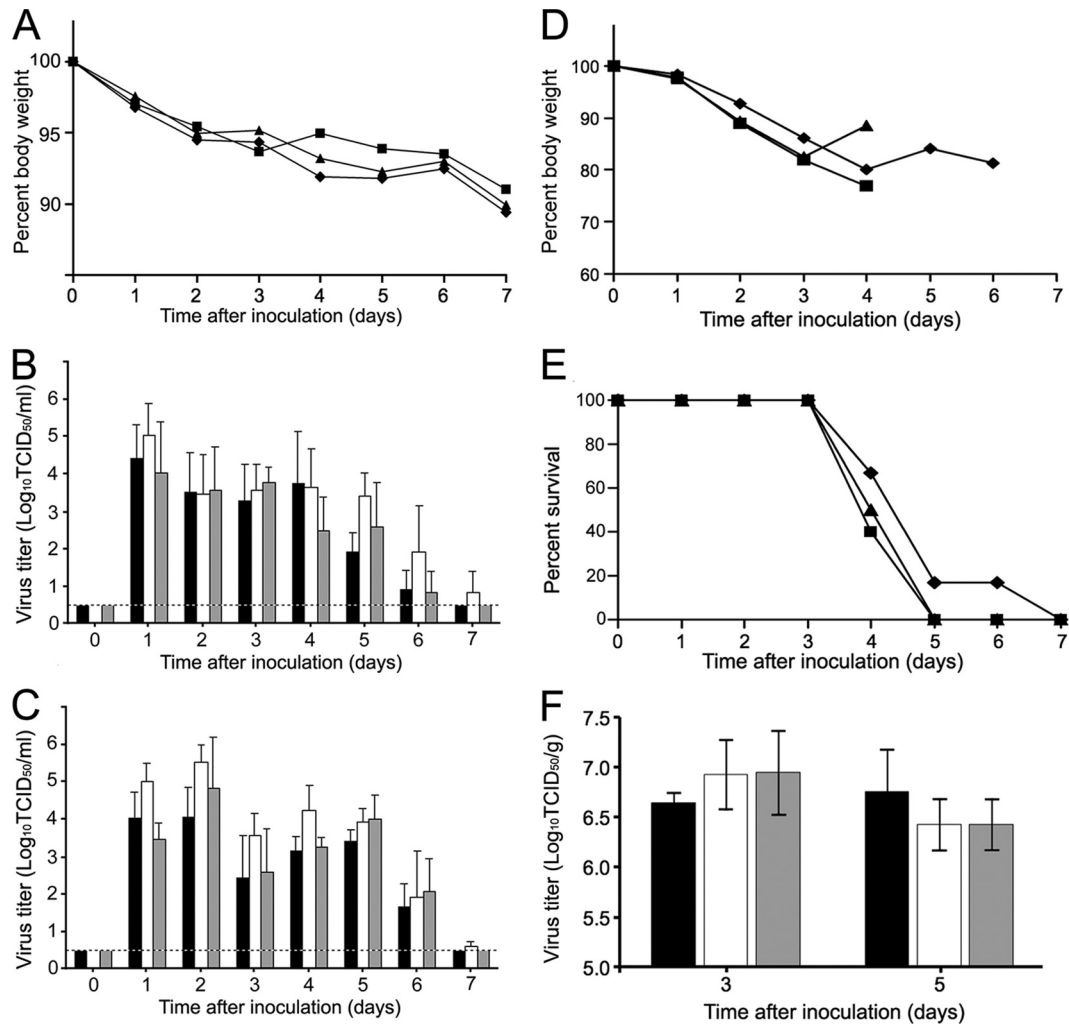


FIG. 1. Weight loss and virus shedding in ferrets and mice inoculated with NL602-WT, NL602-D222E, or NL602-D222G. Data are shown for ferrets (A to C) and mice (D to F) inoculated with NL602-WT (■), NL602-D222E (◆), or NL602-D222G (▲). Body weights are depicted as the percentage of body weight at time of inoculation. Body weight is shown as average for six ferrets until 3 dpi and three ferrets from 4 to 7 dpi (A) or for five to six mice (D). Virus detection in throat swabs (B) and nose swabs (C) in ferrets are indicated for NL602-WT (■), NL602-D222E (□), and NL602-D222G (▨). Geometric mean titers for positive samples are displayed, and error bars indicate the standard deviations. The lower limit of detection is indicated by the dotted line. The proportion of surviving mice is shown for each group (E). Virus titers in the lungs of inoculated mice ($n = 3$) were determined at 3 and 5 dpi, with the geometric mean titers and standard deviations indicated (F). Symbols and colors are consistent in panels A to F.

allow transmission via aerosols or respiratory droplets (33). The inoculated ferrets started to shed virus at 1 dpi, with virus titers up to 10^6 TCID₅₀/ml in throat and nose swabs (Table 1) (see Fig. S5 in the supplemental material). The naive ferrets

became infected as a result of aerosol or respiratory droplet transmission on 1 day postexposure (dpe) in the NL602-D222E group and on 2 dpe in the NL602-WT and NL602-D222G groups. Transmission was detected in all four animals in the

TABLE 1. Virus titers in the respiratory tracts of ferrets inoculated with NL602-WT, NL602-D222E, or NL602-D222G^a

Tissue	Virus titer (\log_{10} TCID ₅₀ /g of tissue) \pm SD at:					
	3 dpi			7 dpi		
	WT	D222E	D222G	WT	D222E	D222G
NT	6.9 \pm 0.3 (3/3)	7.8 \pm 0.2 (3/3)	6.6 \pm 0.2 (3/3)	4.4 \pm 0.7 (2/3)	ND ^b	2.0 \pm 0.2 (2/3)
Trachea	5.0 \pm 0.7 (3/3)	3.6 \pm 1.4 (3/3)	4.5 \pm 1.2 (3/3)	2.4 (1/3)	4.5 (1/3)	ND
Lung	5.6 \pm 0.9 (3/3)	5.8 \pm 1.0 (3/3)	5.5 \pm 0.5 (3/3)	1.5 (1/3)	ND	ND

^a Three ferrets were euthanized at 3 and 7 dpi each. The virus titers in the nasal turbinates (NT), trachea, and lungs were determined. Virus was not detected in any of the extrarespiratory organs. The detection levels for nasal turbinates, trachea, and lungs were <1.63 , <1.68 , and $<1.25 \log_{10}$ TCID₅₀/g of tissue, respectively. The geometric mean titers of positive samples are given, and the numbers of positive animals are indicated in parentheses. WT, wild type.

^b ND, not detected.

TABLE 2. Receptor specificity of wild-type and mutant viruses as determined in a modified TRBC hemagglutination assay^a

Virus	HA titer (HAU/50 μ l)			
	TRBC	VCNA-TRBC	α 2,3-TRBC	α 2,6-TRBC
VN1194/04(H5N1)	128	0	128	0
NL213/03(H3N2)	128	0	0	128
NL602-WT	256	0	0	128
NL602-D222E	128	0	0	128
NL602-D222G	64	0	0	0

^a Hemagglutination titers are expressed as hemagglutinating units (HAU) with normal TRBCs) TRBCs from which sialic acids were removed with *Vibrio cholerae* neuraminidase (VCNA-TRBC), and TRBCs reconstituted with either α 2,3-SAs or α 2,6-SAs.

NL602-WT and NL602-D222G groups and in all three animals in the NL602-D222E group (in this group one animal died, unrelated to the experiment). Virus was extracted from nose swabs of inoculated and exposed ferrets, and the HA sequence was analyzed. No amino acid substitutions were detected. These results indicate that the D222E or D222G substitutions in HA of NL602 had no detectable effect on transmission between ferrets.

Transmission experiments in guinea pigs. Four guinea pigs were inoculated intranasally with 10^4 TCID₅₀ of NL602-WT or NL602-D222G. At 1 dpi, the cage of each infected guinea pig was placed next to that of one naive animal in order to initiate aerosol or respiratory droplet exposure. Animals were housed in this way for a period of 7 days. The virus titers in nasal washes collected from inoculated and exposed animals were determined. Both viruses were detected in the nasal washes of inoculated animals at 2 dpi, with virus titers ranging up to 3×10^8 PFU/ml. All four animals in both groups of exposed animals were infected at 3 dpe (see Fig. S6 in the supplemental material). Thus, introduction of the substitution D222G in HA of NL602 had no detectable effect on transmissibility of the virus via aerosol or respiratory droplets in guinea pigs.

Receptor specificity in hemagglutination assays with modified TRBC. The receptor specificity of wild-type and mutant recombinant viruses was determined by using hemagglutination assays with normal TRBCs or with TRBCs with only α 2,3-SAs or α 2,6-SAs on the cell surface. Removal of sialic acids and proper resialylation of TRBCs were confirmed in hemagglutination assays using the seasonal human H3N2 influenza virus A/Netherlands/213/03 and the avian H5N1 influenza virus A/Viet nam/1194/04. NL602-WT, NL602-D222E, and NL602-D222G had hemagglutination titers of 256, 128, and 64, respectively, using normal TRBCs. After removal of sialic acids from the TRBCs with *Vibrio cholerae* neuraminidase (VCNA), this agglutinating activity was totally abolished. Upon reconstitution of TRBCs with α 2,3-SAs using α 2,3-(N)-sialyltransferase, none of the pdmH1N1 caused hemagglutination, whereas the control avian H5N1 virus caused normal agglutination (Table 2). Upon reconstitution of TRBCs with α 2,6-SAs using α 2,6-(N)-sialyltransferase, NL602-WT and NL602-D222E had hemagglutination titers within 2-fold from titers obtained with untreated TRBCs, as did the control human H3N2 influenza virus (Table 2). In contrast, NL602-D222G did not agglutinate α 2,6-TRBCs. From this experiment, it was concluded that the receptor specificity of NL602-D222G

was different from the receptor specificity of NL602-WT and NL602-D222E. Presumably, NL602-D222G binds to relatively complex sialic acids on TRBCs, in particular sialic acids that were not reconstituted with either α 2,3-(N)-sialyltransferase or α 2,6-(N)-sialyltransferase alone.

Attachment of viruses to cells of mallard duck colon. Next, the receptor specificity of NL602-D222G was compared to that of NL602-WT and NL602-D222E using virus histochemistry (Fig. 2A) (see Fig. S7 in the supplemental material). In this technique, virus attachment to specific tissues is directly visualized using FITC-labeled viruses and formalin-fixed tissue samples. In contrast to NL602-WT and NL602-D222E, NL602-D222G attached abundantly to the epithelial cells of mallard duck colon. It is well known that cells of duck colon express α 2,3-SAs abundantly, both *N*-acetylneuraminic acid (NeuAc α 2,3Gal) and *N*-glycolylneuraminic acid (NeuGc α 2,3Gal) (20). Thus, in contrast to NL602-WT and NL602-D222E, NL602-D222G likely attached to α 2,3-SAs.

Attachment of viruses to cells of the human respiratory tract. Next, the attachment pattern of NL602-WT and NL602-D222G to tissues of the human upper and lower respiratory tracts, including the nasal turbinates, trachea, bronchus, bronchiole, and alveoli, were determined. There were no marked differences in the attachment of the two viruses to cells in the human upper respiratory tract; both viruses attached to ciliated epithelial cells, goblet cells, and the submucosal glands of nasal turbinates (Fig. 2B). In tissues of the human lower respiratory tract, both viruses attached to the epithelium—predominantly ciliated cells—of the trachea, bronchi, and bronchioles, with no marked differences in attachment (Fig. 2C). Interestingly, NL602-D222G attached more abundantly to the intracellular mucus of submucosal glands of the trachea and bronchi than NL602-WT (Fig. 2D) (see Fig. S8 in the supplemental material). In the alveoli, both viruses attached predominantly to type I pneumocytes (Table 3). However, an additional notable difference in the attachment pattern of NL602-WT and NL602-D222G to human respiratory tract tissues was that NL602-D222G attached to a higher proportion of alveolar macrophages and type II pneumocytes in the alveoli (Fig. 2E). This was analyzed quantitatively in alveolar tissues from three individuals by counting positive and negative cells; NL602-D222G attached to 63% of the type II pneumocytes and 53% of the macrophages present in the alveoli, compared to 21 and 11%, respectively, for NL602-WT (Table 3). The higher proportion of positive type II pneumocytes and alveolar macrophages upon incubation with NL602-D222G was consistent among tissues of the three individuals tested (see Table S2 in the supplemental material). Thus, the receptor specificity of NL602-D222G was markedly different from the receptor specificity of NL602-WT, with clear differences in virus attachment to type II pneumocytes and alveolar macrophages in the human respiratory tract.

Structural determinants of α 2,6-linked sialic acid binding. It has previously been reported that the introduction of D222G in HA of 1918 virus resulted in increased binding to α 2,3-SAs and reduced binding to α 2,6-SAs in glycan arrays (47). The pdmH1N1 virus with D222G also bound more abundantly to avian receptors based on virus histochemistry (see Fig. S7 in the supplemental material), yet this was not associated with a loss in binding to receptors present on human cells (Fig. 2). To attempt to explain this potential discrepancy in binding of the

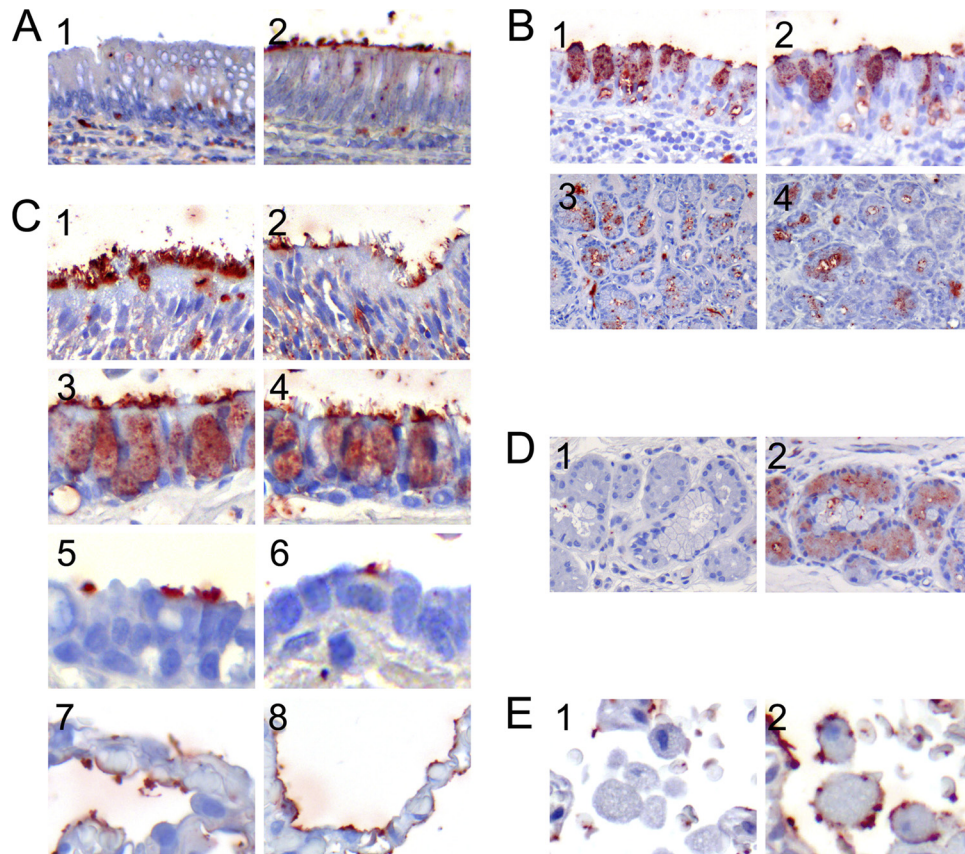


FIG. 2. Attachment of NL602-WT and NL602-D222G viruses to avian and human tissues. The attachment patterns to cells in mallard duck colon (A), human upper respiratory tract (B), and human lower respiratory tract (C to E) are shown. The following tissues were analyzed: colon (A1 and A2), surface epithelium (B1 and B2) and submucosal glands (B3 and B4) of nasal turbinates, trachea (C1 and C2); bronchus (C3 and C4), bronchiole (C5 and C6), alveolus (C7 and C8), tracheal submucosal glands (D1 and D2), and alveolar macrophages (E1 and E2). Virus attachment is shown in red. Odd and even numbers show staining with NL602-WT and NL602-D222G, respectively. The panels were chosen to represent attachment patterns in the whole tissue section as much as possible, but small differences between the single panels and overall view may exist.

two different H1N1 virus mutants to $\alpha 2,6$ -SAs, computer simulations were performed for the 1918 HA and pdmH1N1 HA structures with or without D222G. For 1918 H1N1, $\alpha 2,6$ -SA was observed to bind in two distinct conformations, which we refer to as modes 1 (53% of structures) and 2 (46% of structures). These modes differ in the interactions formed between $\alpha 2,6$ -SA and HA, which change the position of the galactose sugar within the receptor binding pocket (Fig. 3A) (see Fig. S9 in the supplemental material). NL602-WT was also observed to adopt similar binding modes 1 (55% of structures) and 2 (27% of structures) (Fig. 3B) (see Fig. S10 in the supplemental

material). Unlike 1918-WT, many intermediate structures were observed for NL602-WT (Fig. 3C and D, solid lines). The interactions between $\alpha 2,6$ -SA and residues that are different between 1918 and NL602, or that are known to be involved in binding, were monitored throughout the simulations. The most common interactions with $\alpha 2,6$ -SA seen in the simulations of 1918-WT and NL602-WT involved the side chains of 187D and 219K, and both the side chain and backbone of 222D (Fig. 4A and C). For NL602-WT, additional interactions are seen between $\alpha 2,6$ -SA and the side chains of 130K and 142K.

In the simulations for 1918-D222G, $\alpha 2,6$ -SA was observed to

TABLE 3. Virus attachment to cells of the human respiratory tract

Virus	Score ^a and cell type											
	Nasal turbinate		Trachea		Bronchus		Bronchiole		Alveolus			
	Score	Cell type	Score	Cell type	Score	Cell type	Score	Cell type	Score	Cell type	% Type II ^b	% M ϕ
NL602-WT	+*†	C	+/-	C	++*†	C	+	C	++	I	21	11
NL602-D222G	+*†	C	+/-†	C	++*†	C	+	C	++	I	63	53

^a For the score, attachment as shown in Fig. 2 was scored as follows: attachment to no (-), few (+/-), a moderate number (+), or many (++) cells. The median scores for tissues of three individuals are shown. *, The goblet cells were occasionally positive; †, the submucosal glands were positive. Cell type refers to the predominant cell type to which the virus indicated is attached: ciliated cells (C), type I pneumocytes (I), or type II pneumocytes (II).

^b That is, the percent positive type II pneumocytes and alveolar macrophages (M ϕ) in tissues from three individuals were determined, and the averages are given.

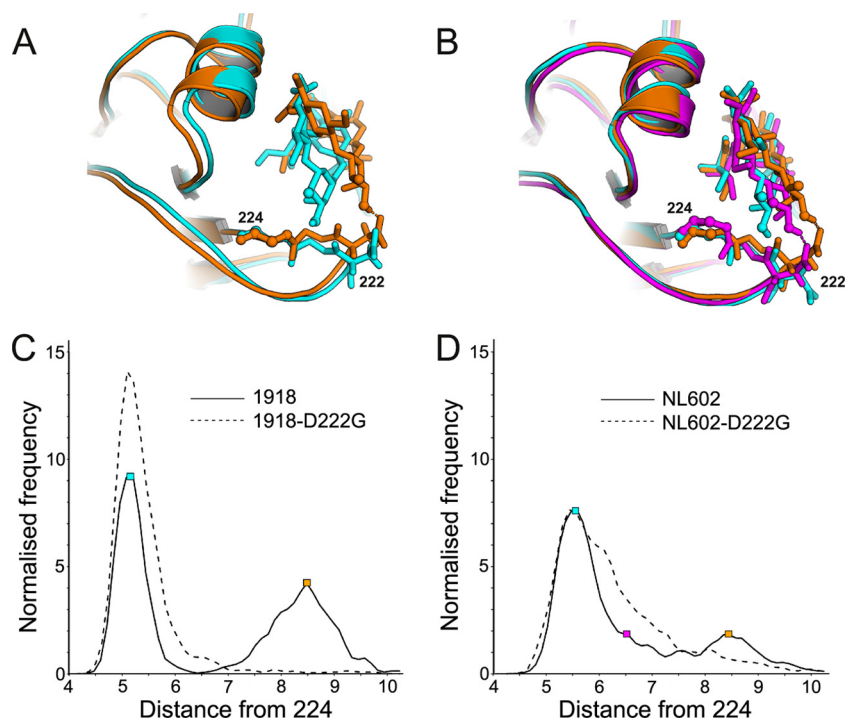


FIG. 3. Representative structures for binding mode 1 (cyan), mode 2 (orange), and intermediate mode (magenta) for 1918 (A) and NL602 (B). All of the structures from the molecular dynamics simulations were classified as mode 1, mode 2, or intermediate based upon the distance between the backbone atoms of residue 224 and the O2 and O3 oxygen atoms of the galactose sugar. These atoms are shown as spheres. Interactions between α 2,6-SA and the side chain of D222 are shown as dashes. Normalized frequency distributions of these distances are shown for the 1918-WT (C) and NL602-WT (D) strains as solid lines, with the D222G mutants shown as dashed lines. For these plots, the frequency was sampled every 0.1 Å. The positions of the representative structures shown in panels A and B are highlighted in these distributions by squares of the corresponding color.

form interactions less frequently with the side chains of 222G and K219 (Fig. 4B and D). These are key to the stability of mode 2 (see Fig. S9C and S9D in the supplemental material), which is seen to be almost entirely lost (Fig. 3C, dashed line). This observation offers an explanation for the reduced binding seen for 1918-D222G (26). For NL602-D222G, this decrease was also observed in the simulations; however, there were additional interactions with the side chains of 130K, 142K, and 224E, which are not present in 1918-D222G. These additional interactions (see Fig. S10C and S10D in the supplemental material) prevent the destabilization of mode 2 in NL602-D222G (Fig. 3D, dashed line). We propose that it is these differences that allow NL602-D222G to maintain binding to α 2,6-SA.

Antigenic properties of wild-type and mutant viruses. The antigenic properties of NL602-WT, NL602-D222E, and NL602-D222G were determined by HI assays using a panel of ferret and rabbit antisera raised against H1 influenza viruses. The antigenic properties of NL602-WT, NL602-D222E, and NL602-D222G were indistinguishable, and substitution D222G thus did not affect the antigenic properties of pdmH1N1 (see Table S3 in the supplemental material).

DISCUSSION

As of January 2010, the public sequence databases contain around 3,000 partial or full-length hemagglutinin sequences for pdmH1N1. In part, these intensive sequencing efforts were

dedicated to screen for the emergence of virulence markers in the pdmH1N1 genome. There have been no indications of the presence of virulence markers in HA to date, with the exception of D222G. Of all HA sequences spanning position 222, close to 92% had 222D, 5.5% had 222E, and 1.4% had 222G, and for 1.3% the amino acid residue at position 222 was uncertain. It has been reported that D222G may arise upon passage of swine influenza A viruses with 222D in embryonated chicken eggs (49). The proportion of sequences with ambiguity at position 222 and sequences with 222G could be related to viral mutants or quasispecies emerging either *in vivo* or upon propagation in eggs. Therefore, the prevalence of 222G in pdmH1N1s in the population cannot be interpreted with certainty using public sequence databases alone. However, in numerous cases of severe disease or fatality due to pdmH1N1 infection, virus genomes with D222G were detected in respiratory specimens by direct sequencing, or upon propagation in cell cultures only (6, 23, 31, 38). A further complication of estimating the true prevalence of 222G in mild and severe cases of disease is the potential bias toward more frequent sampling from the lower respiratory tract in severe cases. Although in one study (23) the virus sequences in the upper and lower respiratory tracts were identical, another study (6) showed that D222G quasispecies were identified mainly in endotracheal aspirate samples and were identified less frequently in nasopharyngeal aspirate samples from patients with severe disease.

The virulence and virus secretion patterns for pdmH1N1

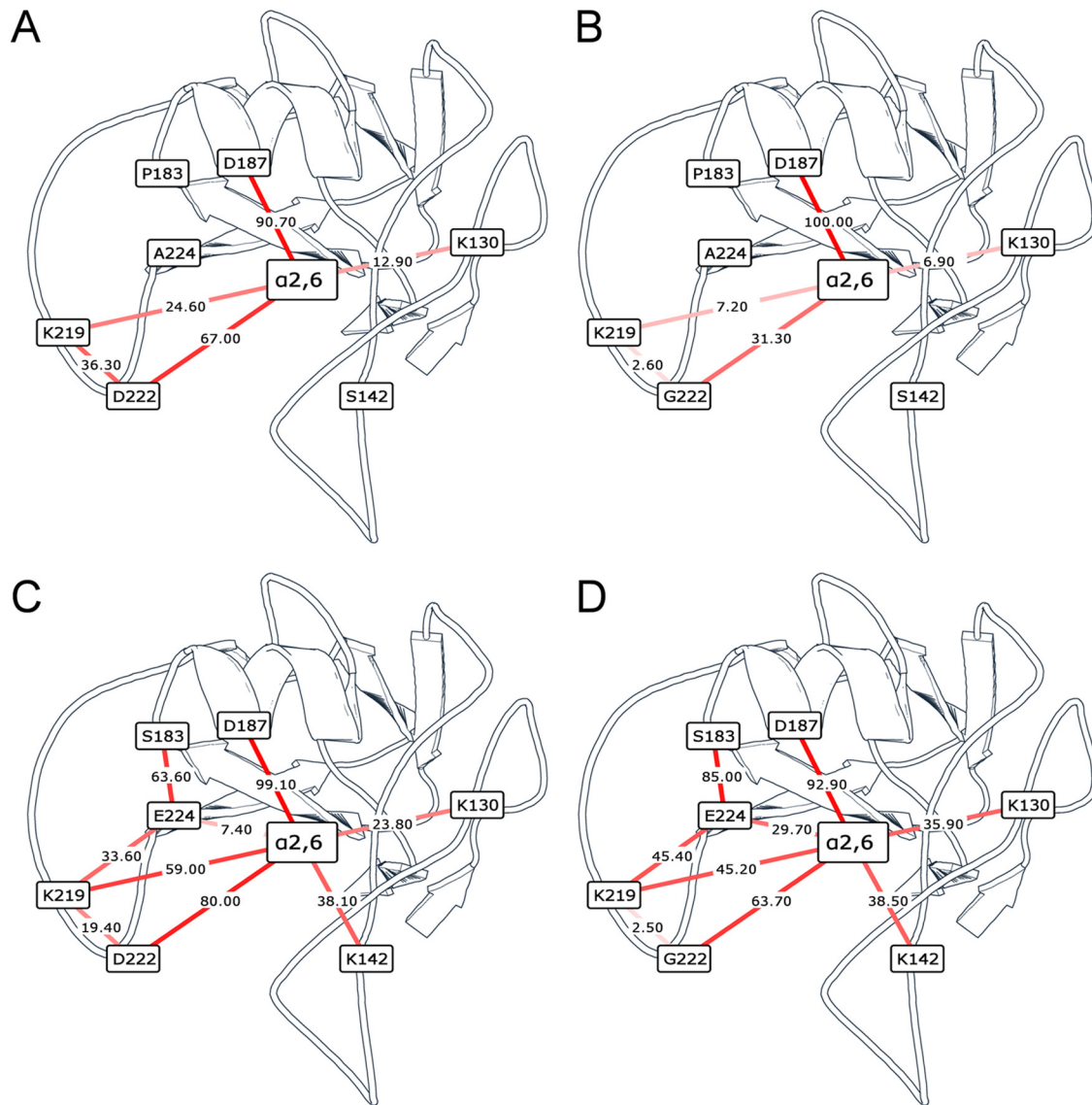


FIG. 4. Set of hydrogen bond interactions within the HA receptor binding site for 1918 (A), 1918-D222G (B), NL602 (C), and NL602-D222G (D). The frequency with which each hydrogen bond is observed in all structures from the molecular dynamics simulations is shown as a percentage and by the depth of color of the connecting lines.

with D222G were comparable to that of wild-type virus in mice and ferrets. The only noticeable difference in pathogenesis was the ocular disease caused by the NL602-D222G virus in mice. Although ocular disease to our knowledge has not been reported as a prominent disease symptom for pdmH1N1 in humans, this trait could point to altered receptor specificity of the D222G virus. To investigate the ocular disease further, mice were inoculated with a lower dose (2.5×10^4 TCID₅₀/mouse) of NL602-WT or NL602-D222G, and none of these mice suffered from ocular disease. Furthermore, virus attachment studies using NL602-WT and NL602-D222G were performed on the eyes and eyelids obtained at necropsy from noninfected mice. This analysis did not show virus attachment to mouse conjunctivae (see Fig. S11 in the supplemental material). Based on these experiments we conclude that the ocular disease was not related to major differences in virus attachment to

mouse conjunctiva, was primarily related to the high inoculum dose used in the pathogenesis experiment, and did not correspond with extensive virus replication in the eyes. These experiments do not exclude the possibility of NL602-D222G attaching to mouse conjunctiva with low affinity, especially when inoculated at a high dose. The absence of purulent exudate from the eyes, as well as the reisolation of NL602-D222G from the eyes of one of three mice tested, suggests that the cause of the observed ocular disease is due to the inoculated virus rather than to another etiological agent such as a bacterium.

The most remarkable difference in phenotype between wild-type and D222G pdmH1N1 was the receptor binding, as revealed by virus attachment studies *in vitro* using tissues of the human respiratory tract, avian colon, and TRBCs. NL602-D222G attached to the same cell types of the human respiratory tract to which NL602-WT attached but also attached more

abundantly to the intracellular mucus of the submucosal glands of the trachea and bronchi and to a higher proportion of macrophages and type-II pneumocytes in the alveoli. Efficient attachment to type II pneumocytes and alveolar macrophages has previously been reported for fatal HPAI H5N1 and H7N7 viruses (34, 52). Such attachment patterns are in agreement with the distribution of α 2,3-SAs in the human respiratory tract (43) and correspond to pathological findings in influenza patients with severe lower respiratory disease (53). It has also been shown that HPAI H5N1 viruses are potent inducers of proinflammatory cytokines in macrophages (7), and it was suggested that this cytokine induction may relate to the unusual disease severity caused by HPAI H5N1 viruses in humans. The abundant attachment of D222G pdmH1N1 to alveolar macrophages may imply that similar mechanisms increase its pathogenicity. In addition, targeting of type II pneumocytes in the alveoli may lead to abundant virus production at these sites, potentially resulting in impaired cell function, including disrupted repair of the epithelium after alveolar damage, disregulated ion transport, and aberrant surfactant production.

In agreement with increased attachment of NL602-D222G to avian cells, the differences in attachment are likely explained by an increased affinity for α 2,3-SAs, while maintaining specificity for α 2,6-SAs. Previous work using glycan arrays with HA of two 1918 H1N1 viruses indicated that D222G increased the affinity for α 2,3-SAs, specifically those with a negative charge such as a sulfate group or sialic acid (47). Although D222G in 1918 HA did not abolish binding to α 2,6-SAs in hemagglutination assays with modified chicken red blood cells, it did result in reduced affinity for a broad range of α 2,6-SAs in glycan arrays (14, 47). In computer simulations, the 1918 HA only formed a limited number of hydrogen bonds to α 2,6-SA. In 1918-D222G, these bonds were weakened such that binding to simple α 2,6-linked glycans would be expected to decrease significantly. In contrast, the HA of NL602-WT formed additional hydrogen bonds to α 2,6-SA via 130K and 142K. These were maintained in NL602-D222G, along with an increase in hydrogen bond interactions between 224E and α 2,6-SA. This observation suggests that these interactions, which were not seen in 1918, allow continued α 2,6 binding in NL602-D222G. It was also shown previously that 1918 virus with 222G bound efficiently to the sulfated sialic acid 6-O-Su-3'-SLN, a glycan found in human airway mucins (25). This observation is in agreement with the binding of NL602-D222G to the submucosal glands in human trachea and bronchi. Whether this attachment reflects a biologically relevant function, related to virus distribution and shedding in humans, remains unknown. Based on the experiments with modified TRBCs, we speculate that the NL602-D222G binds to complex SA receptors, because this virus agglutinated unmodified TRBCs but not reconstituted α 2,3-TRBCs or α 2,6-TRBCs. The simplest explanation for this observation is that the α 2,3-sialyltransferase and α 2,6-sialyltransferase used to reconstitute sialic acids only recognize galactose linked to other glycans via β -1,4 and β -1,3 and that complex sugar molecules, such as those with both α 2,3- and α 2,6-linked structures, were not reconstituted in these assays. Further experiments are required to identify the exact biologically relevant glycans recognized by pdmH1N1 HA with or without D222G.

Although NL602-D222G acquired the ability to bind to

α 2,3-SAs, it retained affinity for α 2,6-SAs associated with attachment and replication in cells of the upper respiratory tract. This observation was in agreement with the D222G virus being transmitted via aerosol or respiratory droplets in animals. In humans, the D222G mutation was identified in a severely ill man and was transmitted to a family member who had only a mild illness (38), which is in agreement with the data presented here indicating that transmission is plausible.

It is further important to note that substitution D222G did not affect the antigenic properties of pdmH1N1, as determined by HI assays with ferret and rabbit antisera; when a panel of antisera against H1 viruses was used, the antigenic properties of NL602-WT and NL602-D222G were indistinguishable (see Table S3 in the supplemental material). These data suggest that currently available pandemic influenza vaccines would provide similar protection to the pdmH1N1s with or without D222G and that vaccination could potentially limit the impact of viruses with D222G in the future.

ACKNOWLEDGMENTS

We thank Peter van Run, Lonneke Leijten, Erin M. Sorrell, Geert van Amerongen, Dennis de Meulder, Dennis Akkermans, and Robert Dias-D'Ullois for technical assistance and Emmie de Wit and Vincent Munster for designing pathogenesis and transmission models.

This study was financed through NIAID-NIH contract HHSN266200700010C and by the European Union FP7 European Management Platform for Emerging and Re-emerging Infectious Disease Entities (EMPERIE) project (223498). D.J.S. and D.F.B. were supported by NIH Director's Pioneer Award DP1-OD000490-01. C.A.R. thanks the HFSP for support, and C.S.W. and D.J.W. thank the EPSRC for support.

REFERENCES

1. Bayly, C. I., P. Cieplak, W. D. Cornell, and P. A. Kollman. 1993. A well-behaved electrostatic potential based method using charge restraints for deriving atomic charges: the RESP model. *J. Phys. Chem.* **97**:10269–10280.
2. Calleja, M., L. Blanshard, R. Bruin, C. Chapman, A. Thandavan, R. Tyer, P. Wilson, V. Alexandrov, R. J. Allen, J. Brodholt, M. T. Dove, W. Emmerich, and K. Kleese van Dam. 2004. Grid tool integration within the eMinerals project. Proceedings of the UK e-Science All Hands Meeting 2004. ISBN 1904425216:812–817.
3. Cao, B., X. W. Li, Y. Mao, J. Wang, H. Z. Lu, Y. S. Chen, Z. A. Liang, L. Liang, S. J. Zhang, B. Zhang, L. Gu, L. H. Lu, D. Y. Wang, C. Wang, and the National Influenza A Pandemic (H1H1) 2009 Clinical Investigation Group of China. 2009. Clinical features of the initial cases of 2009 pandemic influenza A (H1N1) virus infection in China. *N. Engl. J. Med.* **361**:2507–2517.
4. Case, D. A., T. A. Darden, I. Cheatham, C. L. Simmerling, J. Wang, R. E. Duke, R. Luo, M. Crowley, R. C. Walker, W. Zhang, K. M. Merz, B. Wang, S. Hayik, A. Roitberg, G. Seabra, I. Kolosváry, K. F. Wong, F. Paesani, J. Vanicek, X. Wu, S. R. Brozell, T. Steinbrecher, H. Gohlke, L. Yang, C. Tan, J. Mongan, V. Hornak, G. Cui, D. H. Mathews, M. G. Seetin, C. Sagui, V. Babin, and P. A. Kollman. 2008. AMBER 10. University of California, San Francisco.
5. Chen, G. W., and S. R. Shih. 2009. Genomic signatures of influenza A pandemic (H1N1) 2009 virus. *Emerg. Infect. Dis.* **15**:1897–1903.
6. Chen, H., X. Wen, K. K. To, P. Wang, H. Tse, J. F. Chan, H. W. Tsoi, K. S. Fung, C. W. Tse, R. A. Lee, K. H. Chan, and K. Y. Yuen. 2010. Quasispecies of the D225G substitution in the hemagglutinin of pandemic influenza A (H1N1) 2009 virus from patients with severe disease in Hong Kong, China. *J. Infect. Dis.* **201**:1517–1521.
7. Cheung, C. Y., L. L. Poon, A. S. Lau, W. Luk, Y. L. Lau, K. F. Shortridge, S. Gordon, Y. Guan, and J. S. Peiris. 2002. Induction of proinflammatory cytokines in human macrophages by influenza A (H5N1) viruses: a mechanism for the unusual severity of human disease? *Lancet* **360**:1831–1837.
8. Conenello, G. M., D. Zamarin, L. A. Perrone, T. Tumpey, and P. Palese. 2007. A single mutation in the PB1-F2 of H5N1 (HK/97) and 1918 influenza A viruses contributes to increased virulence. *PLoS Pathog.* **3**:1414–1421.
9. Dawood, F. S., S. Jain, L. Finelli, M. W. Shaw, S. Lindstrom, R. J. Garten, L. V. Gubareva, X. Xu, C. B. Bridges, and T. M. Uyeki. 2009. Emergence of a novel swine-origin influenza A (H1N1) virus in humans. *N. Engl. J. Med.* **360**:2605–2615.
10. de Wit, E., M. I. Spronken, T. M. Bestebroer, G. F. Rimmelzwaan, A. D.

- Osterhaus, and R. A. Fouchier. 2004. Efficient generation and growth of influenza virus A/PR/8/34 from eight cDNA fragments. *Virus Res.* **103**:155–161.
11. Donaldson, L. J., P. D. Rutter, B. M. Ellis, F. E. Greaves, O. T. Mytton, R. G. Pebody, and I. E. Yardley. 2009. Mortality from pandemic A/H1N1 2009 influenza in England: public health surveillance study. *BMJ* **339**:b5213.
 12. Fraser, C., C. A. Donnelly, S. Cauchemez, W. P. Hanage, M. D. Van Kerkhove, T. D. Hollingsworth, J. Griffin, R. F. Baggaley, H. E. Jenkins, E. J. Lyons, T. Jombart, W. R. Hinsley, N. C. Grassly, F. Balloux, A. C. Ghani, N. M. Ferguson, A. Rambaut, O. G. Pybus, H. Lopez-Gatell, C. M. Alpujch-Aranda, I. B. Chapela, E. P. Zavala, D. M. Guevara, F. Checchi, E. Garcia, S. Hugonnet, C. Roth, et al. 2009. Pandemic potential of a strain of influenza A (H1N1): early findings. *Science* **324**:1557–1561.
 13. Garten, R. J., C. T. Davis, C. A. Russell, B. Shu, S. Lindstrom, A. Balish, W. M. Sessions, X. Xu, E. Skepner, V. Deyde, M. Okomo-Adhiambo, L. Gubareva, J. Barnes, C. B. Smith, S. L. Emery, M. J. Hillman, P. Rivaviller, J. Smagala, M. de Graaf, D. F. Burke, R. A. Fouchier, C. Pappas, C. M. Alpujch-Aranda, H. Lopez-Gatell, H. Olivera, I. Lopez, C. A. Myers, D. Faix, P. J. Blair, C. Yu, K. M. Keene, P. D. Dotson, Jr., D. Boxrud, A. R. Sambol, S. H. Abid, K. St. George, T. Bannerman, A. L. Moore, D. J. Stringer, P. Blevins, G. J. Demmler-Harrison, M. Ginsberg, P. Kriner, S. Waterman, S. Smole, H. F. Guevara, E. A. Belongia, P. A. Clark, S. T. Beatrice, R. Donis, J. Katz, L. Finelli, C. B. Bridges, M. Shaw, D. B. Jernigan, T. M. Uyeki, D. J. Smith, A. I. Klimov, and N. J. Cox. 2009. Antigenic and genetic characteristics of swine-origin 2009 A(H1N1) influenza viruses circulating in humans. *Science* **325**:197–201.
 14. Glaser, L., J. Stevens, D. Zamarin, I. A. Wilson, A. Garcia-Sastre, T. M. Tumpey, C. F. Basler, J. K. Taubenberger, and P. Palese. 2005. A single amino acid substitution in 1918 influenza virus hemagglutinin changes receptor binding specificity. *J. Virol.* **79**:11533–11536.
 15. Hai, R., M. Schmolke, Z. T. Varga, B. Manicassamy, T. T. Wang, J. A. Belsler, M. B. Pearce, A. Garcia-Sastre, T. M. Tumpey, and P. Palese. 2010. PB1-F2 expression by the 2009 pandemic H1N1 influenza virus has minimal impact on virulence in animal models. *J. Virol.* doi:10.1128/JVI.02717–09.
 16. Hale, B. G., J. Steel, B. Manicassamy, R. A. Medina, J. Ye, D. Hickman, A. C. Lowen, D. R. Perez, and A. Garcia-Sastre. 2010. Mutations in the NS1 C-terminal tail do not enhance replication or virulence of the 2009 pandemic H1N1 influenza A virus. *J. Gen. Virol.* doi:10.1099/vir.0.020925-0.
 17. Hatta, M., P. Gao, P. Halfmann, and Y. Kawaoka. 2001. Molecular basis for high virulence of Hong Kong H5N1 influenza A viruses. *Science* **293**:1840–1842.
 18. Herfst, S., S. Chutinimitkul, J. Ye, E. de Wit, V. J. Munster, E. J. Schrauwen, T. M. Bestebroer, M. Jonges, A. Meijer, M. Koopmans, G. F. Rimmelzwaan, A. D. Osterhaus, D. R. Perez, and R. A. Fouchier. 2010. Introduction of virulence markers in PB2 of pandemic swine-origin influenza virus does not result in enhanced virulence or transmission. *J. Virol.* doi:10.1128/JVI.02634–09.
 19. Hoffmann, E., G. Neumann, Y. Kawaoka, G. Hobom, and R. G. Webster. 2000. A DNA transfection system for generation of influenza A virus from eight plasmids. *Proc. Natl. Acad. Sci. U. S. A.* **97**:6108–6113.
 20. Ito, T., Y. Suzuki, T. Suzuki, A. Takada, T. Horimoto, K. Wells, H. Kida, K. Otsuki, M. Kiso, H. Ishida, and Y. Kawaoka. 2000. Recognition of *N*-glycolylneuraminic acid linked to galactose by the α 2,3 linkage is associated with intestinal replication of influenza A virus in ducks. *J. Virol.* **74**:9300–9305.
 21. Jackson, D., M. J. Hossain, D. Hickman, D. R. Perez, and R. A. Lamb. 2008. A new influenza virus virulence determinant: the NS1 protein four C-terminal residues modulate pathogenicity. *Proc. Natl. Acad. Sci. U. S. A.* **105**:4381–4386.
 22. Karber, G. 1931. Beitrag zur kollektiven Behandlung pharmakologischer Reihenversuche. *Arch. Exp. Pathol. Pharmacol.* **162**:480–483.
 23. Kilander, A., R. Rykkvin, S. Dudman, and O. Hungnes. 2010. Observed association between the HA1 mutation D222G in the 2009 pandemic influenza A(H1N1) virus and severe clinical outcome, Norway 2009–2010. *Eur. Surveill.* **15**:19498.
 24. Kirschner, K. N., A. B. Yongye, S. M. Tschempel, J. Gonzalez-Outeirino, C. R. Daniels, B. L. Foley, and R. J. Woods. 2008. GLYCAM06: a generalizable biomolecular force field. *Carbohydr. J. Comput. Chem.* **29**:622–655.
 25. Lamblin, G., S. Degroote, J. M. Perini, P. Delmotte, A. Scharfman, M. Davril, J. M. Lo-Guidice, N. Houdret, V. Dumur, A. Klein, and P. Rousse. 2001. Human airway mucin glycosylation: a combinatorial of carbohydrate determinants which vary in cystic fibrosis. *Glycoconj. J.* **18**:661–684.
 26. Li, Z., H. Chen, P. Jiao, G. Deng, G. Tian, Y. Li, E. Hoffmann, R. G. Webster, Y. Matsuoka, and K. Yu. 2005. Molecular basis of replication of duck H5N1 influenza viruses in a mammalian mouse model. *J. Virol.* **79**:12058–12064.
 27. Libster, R., J. Bugna, S. Coviello, D. R. Hijano, M. Dunaiewsky, N. Reynoso, M. L. Cavalieri, M. C. Guglielmo, M. S. Areso, T. Gilligan, F. Santucho, G. Cabral, G. L. Gregorio, R. Moreno, M. I. Lutz, A. L. Panigasi, L. Saligari, M. T. Caballero, R. M. Egues Almeida, M. E. Gutierrez Meyer, M. D. Neder, M. C. Davenport, M. P. Del Valle, V. S. Santidrian, G. Mosca, M. Garcia Dominguez, L. Alvarez, P. Landa, A. Pota, N. Bolonati, R. Dalamon, V. I. Sanchez Mercol, M. Espinoza, J. C. Peuchot, A. Karolinski, M. Bruno, A. Borsa, F. Ferrero, A. Bonina, M. Ramonet, L. C. Albano, N. Luedicke, E. Alterman, V. Savy, E. Baumeister, J. D. Chappell, K. M. Edwards, G. A. Melendi, and F. P. Polack. 2009. Pediatric hospitalizations associated with 2009 pandemic influenza A (H1N1) in Argentina. *N. Engl. J. Med.* **362**:45–55.
 28. Lindahl, E., B. A. Hess, and D. van der Spoel. 2001. GROMACS 3.0: a package for molecular simulation and trajectory analysis. *J. Mol. Mod.* **7**:306–317.
 29. Louie, J. K., M. Acosta, D. J. Jamieson, M. A. Honein, and G. California Pandemic Working. 2010. Severe 2009 H1N1 influenza in pregnant and postpartum women in California. *N. Engl. J. Med.* **362**:27–35.
 30. Louie, J. K., M. Acosta, K. Winter, C. Jean, S. Gavali, R. Schechter, D. Vugia, K. Harriman, B. Matyas, C. A. Glaser, M. C. Samuel, J. Rosenberg, J. Talarico, D. Hatch, and California Pandemic (H1N1) Working Group. 2009. Factors associated with death or hospitalization due to pandemic 2009 influenza A(H1N1) infection in California. *JAMA* **302**:1896–1902.
 31. Mak, G. C., K. W. Au, L. S. Tai, K. C. Chuang, K. C. Cheng, T. C. Shiu, and W. Lim. 2010. Association of D222G substitution in haemagglutinin of 2009 pandemic influenza A (H1N1) with severe disease. *Eur. Surveill.* **15**:19534.
 32. Matsuoka, Y., D. E. Swayne, C. Thomas, M. A. Rameix-Welti, N. Naffakh, C. Warnes, M. Altholtz, R. Donis, and K. Subbarao. 2009. Neuraminidase stalk length and additional glycosylation of the hemagglutinin influence the virulence of influenza H5N1 viruses for mice. *J. Virol.* **83**:4704–4708.
 33. Munster, V. J., E. de Wit, J. M. van den Brand, S. Herfst, E. J. Schrauwen, T. M. Bestebroer, D. van de Vijver, C. A. Boucher, M. Koopmans, G. F. Rimmelzwaan, T. Kuiken, A. D. Osterhaus, and R. A. Fouchier. 2009. Pathogenesis and transmission of swine-origin 2009 A(H1N1) influenza virus in ferrets. *Science* **325**:481–483.
 34. Munster, V. J., E. de Wit, D. van Riel, W. E. Beyer, G. F. Rimmelzwaan, A. D. Osterhaus, T. Kuiken, and R. A. Fouchier. 2007. The molecular basis of the pathogenicity of the Dutch highly pathogenic human influenza A H7N7 viruses. *J. Infect. Dis.* **196**:258–265.
 35. Nicholls, J. M., R. W. Chan, R. J. Russell, G. M. Air, and J. S. Peiris. 2008. Evolving complexities of influenza virus and its receptors. *Trends Microbiol.* **16**:149–157.
 36. Nobusawa, E., H. Ishihara, T. Morishita, K. Sato, and K. Nakajima. 2000. Change in receptor-binding specificity of recent human influenza A viruses (H3N2): a single amino acid change in hemagglutinin altered its recognition of sialyloligosaccharides. *Virology* **278**:587–596.
 37. Perez-Padilla, R., D. de la Rosa-Zamboni, S. Ponce de Leon, M. Hernandez, F. Quinones-Falconi, E. Bautista, A. Ramirez-Venegas, J. Rojas-Serrano, C. E. Ormsby, A. Corrales, A. Higuera, E. Mondragon, J. A. Cordova-Villalobos, and the INER Working Group on Influenza. 2009. Pneumonia and respiratory failure from swine-origin influenza A (H1N1) in Mexico. *N. Engl. J. Med.* **361**:680–689.
 38. Puzelli, S., M. Facchini, D. Spagnolo, M. A. De Marco, L. Calzetti, A. Zanetti, R. Fumagalli, M. L. Tanzi, A. Cassone, G. Rezza, and I. Donatelli. 2010. Transmission of hemagglutinin D222G mutant strain of pandemic (H1N1) 2009 virus. *Emerg. Infect. Dis.* **16**:863–865.
 39. Rimmelzwaan, G. F., T. Kuiken, G. van Amerongen, T. M. Bestebroer, R. A. Fouchier, and A. D. Osterhaus. 2001. Pathogenesis of influenza A (H5N1) virus infection in a primate model. *J. Virol.* **75**:6687–6691.
 40. Sali, A., and T. L. Blundell. 1993. Comparative protein modeling by satisfaction of spatial restraints. *J. Mol. Biol.* **234**:779–815.
 41. Schmidt, M. W., K. K. Baldrige, J. A. Boatz, S. T. Elbert, M. S. Gordon, J. H. Jensen, S. Koseki, N. Matsunaga, K. A. Nguyen, S. Su, T. L. Windus, M. Dupuis, and J. A. Montgomery. 1993. General atomic and molecular electronic structure system. *J. Comput. Chem.* **14**:1347–1363.
 42. Shinde, V., C. B. Bridges, T. M. Uyeki, B. Shu, A. Balish, X. Xu, S. Lindstrom, L. V. Gubareva, V. Deyde, R. J. Garten, M. Harris, S. Gerber, S. Vagasky, F. Smith, N. Pascoe, K. Martin, D. Dufficy, K. Ritger, C. Conover, P. Quinlisk, A. Klimov, J. S. Bresse, and L. Finelli. 2009. Triple-reassortant swine influenza A (H1) in humans in the United States, 2005–2009. *N. Engl. J. Med.* **360**:2616–2625.
 43. Shinya, K., M. Ebina, S. Yamada, M. Ono, N. Kasai, and Y. Kawaoka. 2006. Avian flu: influenza virus receptors in the human airway. *Nature* **440**:435–436.
 44. Smith, D. J., A. S. Lapedes, J. C. de Jong, T. M. Bestebroer, G. F. Rimmelzwaan, A. D. Osterhaus, and R. A. Fouchier. 2004. Mapping the antigenic and genetic evolution of influenza virus. *Science* **305**:371–376.
 45. Smith, R. E., S. C. Lovell, D. F. Burke, R. W. Montalvo, and T. L. Blundell. 2007. Andante: reducing side chain rotamer search space during comparative modeling using environment-specific substitution probabilities. *Bioinformatics* **23**:1099–1105.
 46. Steel, J., A. C. Lowen, S. Mubareka, and P. Palese. 2009. Transmission of influenza virus in a mammalian host is increased by PB2 amino acids 627K or 627E/701N. *PLoS Pathog.* **5**:e1000252.
 47. Stevens, J., O. Blixt, L. Glaser, J. K. Taubenberger, P. Palese, J. C. Paulson, and I. A. Wilson. 2006. Glycan microarray analysis of the hemagglutinins from modern and pandemic influenza viruses reveals different receptor specificities. *J. Mol. Biol.* **355**:1143–1155.
 48. Subbarao, E. K., W. London, and B. R. Murphy. 1993. A single amino acid

- in the PB2 gene of influenza A virus is a determinant of host range. *J. Virol.* **67**:1761–1764.
49. **Takamae, N., R. Ruttanapumma, S. Parchariyanon, S. Yoneyama, T. Hayashi, H. Hiramatsu, N. Sriwilaijaroen, Y. Uchida, S. Kondo, H. Yagi, K. Kato, Y. Suzuki, and T. Saito.** 2010. Alterations in receptor binding properties of swine influenza viruses of H1 subtype after isolation in embryonated chicken eggs. *J. Gen. Virol.* **91**:938–948.
 50. **Tumpey, T. M., T. R. Maines, N. Van Hoeven, L. Glaser, A. Solorzano, C. Pappas, N. J. Cox, D. E. Swayne, P. Palese, J. M. Katz, and A. Garcia-Sastre.** 2007. A two-amino acid change in the hemagglutinin of the 1918 influenza virus abolishes transmission. *Science* **315**:655–659.
 51. **Van Hoeven, N., C. Pappas, J. A. Belser, T. R. Maines, H. Zeng, A. Garcia-Sastre, R. Sasisekharan, J. M. Katz, and T. M. Tumpey.** 2009. Human HA and polymerase subunit PB2 proteins confer transmission of an avian influenza virus through the air. *Proc. Natl. Acad. Sci. U. S. A.* **106**:3366–3371.
 52. **van Riel, D., V. J. Munster, E. de Wit, G. F. Rimmelzwaan, R. A. Fouchier, A. D. Osterhaus, and T. Kuiken.** 2006. H5N1 virus attachment to lower respiratory tract. *Science* **312**:399.
 53. **van Riel, D., V. J. Munster, E. de Wit, G. F. Rimmelzwaan, R. A. Fouchier, A. D. Osterhaus, and T. Kuiken.** 2007. Human and avian influenza viruses target different cells in the lower respiratory tract of humans and other mammals. *Am. J. Pathol.* **171**:1215–1223.
 54. **Wales, D. J.** 2010. GMIN. <http://www.wales.ch.cam.ac.uk/software.html>. Updated 19 February 2010. Accessed 19 February 2010.
 55. **Wales, D. J., and J. P. K. Doye.** 1997. Global optimization by Basin-Hopping and the lowest energy structures of Lennard-Jones clusters containing up to 110 atoms. *J. Phys. Chem.* **101**:5111–5116.
 56. **World Health Organization.** 2009. Public health significance of virus mutation detected in Norway pandemic (H1N1) 2009. http://www.who.int/csr/disease/swineflu/notes/briefing_20091120/en/. Accessed 28 April 2010.